

Multiple Moving Cracks in an Orthotropic Strip Sandwiched between Two Piezoelectric Layers

M. Nourazar*
M.Sc. Student

M. Ayatollahi†
Associate Professor

In this paper, the solution of a moving Volterra-type screw dislocation in an orthotropic layer, bonded between two piezoelectric layers is obtained using complex Fourier transform. The dislocation solution is then employed as strain nuclei to derive singular integral equations for a medium weakened by multiple moving cracks. These equations, which are classified as, Cauchy singular equations, are then solved numerically for the dislocation densities functions on the crack surfaces. The dislocation densities are employed to determine stress intensity factors for multiple moving cracks. Finally, the effects of the material properties, geometrical parameters and the speed of the crack propagating on the stress intensity factors and strain energy density factor are investigated. It is shown from theses results that the effect of the crack propagation speed can be highly significant.

Keywords: Moving screw dislocation; Multiple cracks; Singular integral equations; Stress intensity factors; Strain energy density factor.

1 Introduction

Dynamic fracture mechanics of layered materials has been gaining lots of attentions among the researchers where the layered materials are extensively used in various products and devices to improve structural performance such as strength and durability. The influence of the crack moving speed on the the stress intensity factors was a popular subject in classical elastodynamics. Among the models of propagating crack, Yoffe crack is the simplest and the most classical one. In this model, a Griffith crack is assumed to propagate straight at a constant speed with its length unchanged. Most of the piezoelectric sensors are layered structures, and the control of laminated structures including piezoelectric devices has been extensively studied in the literature. In a practical application, bonding of piezoelectric layers frequently happens.

The simplest structure is just composed of two piezoelectric layers and a substrate; therefore, the study of the fracture mechanics of the materials composed of piezoelectric layers is very substantial in the design of piezoelectric devices. Orthotropic composites are sometimes used as the substrate of layered piezoelectric devices to enhance mechanical performance. Sih et al. [1] studied the dynamic behavior of a moving crack in layered composites.

* M.Sc. Student, Faculty of Engineering, University of Zanjan, Zanjan, Iran mn_Nourazar@yahoo.com

† Corresponding Author, Associate Professor, Faculty of Engineering, University of Zanjan, Zanjan, Iran mo.ayatollahy@gmail.com

Chen et al. [2] analyzed a Yoffe-type crack along the interface of two dissimilar piezoelectric materials and revealed that the stress and electric displacement intensity factors depend on the moving speed of crack, differing from the case of a single piezoelectric media. The problem of an interface crack between piezoelectric and elastic strips was investigated by Kwon and Lee [3]. Das et al. [4] have solved the problem of propagation of two equal length collinear Griffith cracks in an orthotropic elastic layer of finite thickness sandwiched between two identical orthotropic half-planes. The problem of a finite Griffith crack moving with constant velocity along the interface of a two-layered strip composed of a piezoelectric ceramic and an elastic layers has been discussed by Kwon and Lee [5]. Jiang and Wang [6] made the dynamic analysis of Yoffe type crack propagating in a functionally graded layer bonded to dissimilar half planes. Kwon et al. [7] studied an eccentric crack moving at constant speed in a piezoelectric ceramic strip sandwiched between elastic half-planes under exact permeable condition. The dynamic intensity factor and the dynamic energy release rate have been presented graphically to show the effects of the crack propagation speed as well as the electromechanical coupling coefficient. The problem of an interfacial crack along the interface between a piezoelectric and two orthotropic materials under electromechanical shear loadings was analyzed by Lee et al. [8]. Kwon et al. [9] studied electromechanical behavior of an eccentric crack in a piezoelectric ceramic layer bonded between two elastic layers under anti-plane mechanical and in-plane electrical loadings. The stress intensity factor for cracked multi-layered and functionally graded coatings was obtained by Chi and Chung [10]. A finite crack with constant length propagating in the functionally graded orthotropic strip under in plane loading was investigated by Ma et al. [11].

The effects of material properties, the thickness of the functionally graded orthotropic strip and the speed of the crack propagating upon the dynamic fracture behavior were studied. Das [12], Considered the interaction between three moving collinear Griffith cracks under antiplane shear stress situated at the interface of an elastic layer overlying a different half plane. The finite crack with constant length (Yoffe-type crack) propagating in a functionally graded strip with spatially varying elastic properties between two dissimilar homogeneous layers under in-plane loading was studied by Cheng and Zhong [13]. The multiple crack propagation along the interface of two bonded dissimilar strips are studied by Matbully [14]. Li and Ding [15] determined mode III stress intensity factor for a crack in the functionally graded piezoelectric layer bonded to a piezoelectric half-plane. Feng et al. [16] investigated the problem of multiple cracks on the interface between a piezoelectric layer and orthotropic substrate and showed the stress intensity factor is dependent on the geometrical parameters and material orthotropy. The solution of dynamic crack problem in an functionally graded piezoelectric layer bonded to two piezoelectric strips was given by Shin and Lee [17].

Ding and Li [18] investigated the problem of two collinear cracks perpendicular to the interface of functionally graded orthotropic strip bonded to an orthotropic substrate. They studied the effects of the orthotropy and nonhomogeneous parameters on the stress intensity factors. To the best knowledge of the authors, There are a few analytical studies have been conducted on the moving cracks in multilayer structures.

The objective of this work to determine the stress intensity factors of multiple moving cracks with constant velocity in a three-layered medium composed of an orthotropic strip and two piezoelectric layers. The out-of-plane mechanical load is applied to the medium. Fourier transforms are used to reduce the problem to Cauchy singular integral equations. The resulting singular integral equations are solved using the method, developed by Erdogan and Gupta [19], to provide the dislocation density on the cracks surfaces.

Finally, the stress intensity factors and strain energy density factor are addressed and discussed.

2 Formulation of the problem

We consider an orthotropic layer of thickness h bonded with two piezoelectric layers. Referring to Figure (1), let piezoelectric layer 1 occupy the upper ($y \geq 0$, thickness h_1), while piezoelectric layer 2 occupy the lower ($-(h+h_2) \leq y \leq -h$, thickness h_2) regions. In the orthotropic substrate, principal axes of orthotropy are respectively parallel and normal to the X and Y axes. The boundary value problem is simplified considerably if we consider only the out of-plane displacement and the in-plane electric fields. The constitutive equations for the piezoelectric layers can be written as:

$$\begin{aligned} \sigma_{zx_i}(X,Y) &= c_{44} \frac{\partial W_i}{\partial X} + e_{15} \frac{\partial \phi_i}{\partial X}, \quad \sigma_{zy_i}(X,Y) = c_{44} \frac{\partial W_i}{\partial Y} + e_{15} \frac{\partial \phi_i}{\partial Y}, \\ D_{xi}(X,Y) &= e_{15} \frac{\partial W_i}{\partial X} - d_{11} \frac{\partial \phi_i}{\partial X}, \quad D_{yi}(X,Y) = e_{15} \frac{\partial W_i}{\partial Y} - d_{11} \frac{\partial \phi_i}{\partial Y}, \quad i = 1, 2, \end{aligned} \quad (1)$$

where D_{xi} , D_{yi} and ϕ_i are the components of electric displacements, and electric potential, respectively, c_{44} , e_{15} and d_{11} are material constants. The governing equations of orthotropic strip under anti-plane deformation have the following forms:

$$\sigma_{zx}(X,Y) = G_x \frac{\partial W(X,Y)}{\partial X}, \quad \sigma_{zy}(X,Y) = G_y \frac{\partial W(X,Y)}{\partial Y} \quad -h \leq Y \leq 0 \quad (2)$$

In above equalities, G_x and G_y are the orthotropic shear moduli of elasticity of material. From Eqs. (1) and (2), and by using the equilibrium equations and the Maxwell equation, The governing equations in this problem can be written in the following forms,

$$c_{44} \nabla^2 W_i(X,Y,t) + e_{15} \nabla^2 \phi_i(X,Y,t) = \rho_i \frac{\partial^2 W_i(X,Y,t)}{\partial t^2} \quad (3a)$$

$$e_{15} \nabla^2 W_i(X,Y,t) - d_{11} \nabla^2 \phi_i(X,Y,t) = 0, \quad i = 1, 2 \quad (3b)$$

$$G \frac{\partial^2 W}{\partial X^2} + \frac{\partial^2 W}{\partial Y^2} = \frac{1}{C^2} \frac{\partial^2 W}{\partial t^2}, \quad -h < Y < 0 \quad (3c)$$

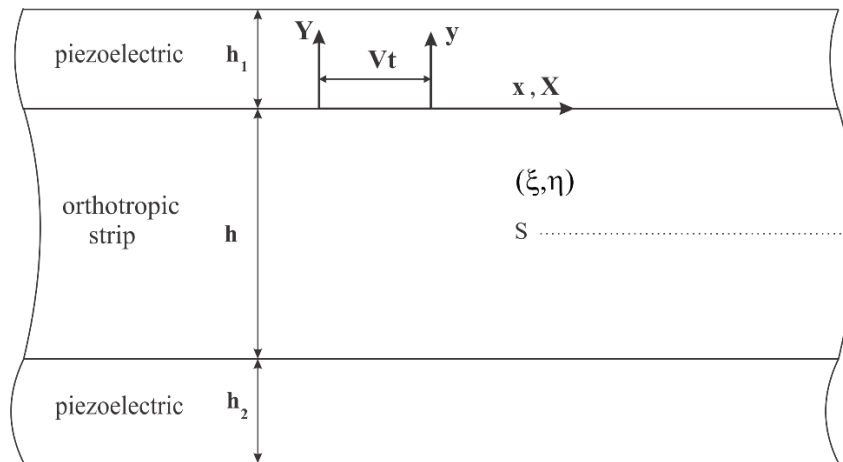


Figure 1 Schematic view of the medium with moving screw dislocation.

where $G = G_x / G_y$ and $C = \sqrt{G_y / \rho}$ is the characteristic elastic shear wave velocity for the orthotropic layer in the Y direction. The governing equations of piezoelectric layers simplify considerably with the use of Bleustein function, i.e.,

$$\psi_i(X, Y, t) = \phi - \alpha W_i(X, Y, t), \quad i = 1, 2 \quad (4)$$

In which $\alpha = e_{15} / d_{11}$, Eqs. (3a,b) can be written as follows:

$$\nabla^3 W_i = \frac{\rho_i}{\tilde{c}_{44}} \frac{\partial^2 W_i}{\partial t^2}, \quad \nabla^2 \psi_i = 0, \quad i = 1, 2, \quad (5)$$

where $\tilde{c}_{44} = c_{44} + (e_{15})^2 / d_{11}$ is the piezoelectric stiffened elastic constant. For the current problem, it is convenient to introduce the following Galilean transformation:

$$X = x + Vt, \quad Y = y, \quad \frac{\partial}{\partial t} = -V \frac{\partial}{\partial x}. \quad (6)$$

where (x, y) is the translating coordinate system attached to the moving dislocation.

The dislocation is characterized by Burger vector b_{wz} , and moving with uniformly subsonic velocity V in the horizontal direction. It is, however, assumed that the propagation of the crack has prevailed for such along time that the stress distribution around its tip is time invariant in the translating reference frame. In the transformed coordinate system, Eqs. (3) can be written based on the moving coordinate system as:

$$\Gamma^2 \frac{\partial^2 w_i}{\partial x^2} + \frac{\partial^2 w_i}{\partial y^2} = 0, \quad (7a)$$

$$\frac{\partial^2 \psi_i}{\partial x^2} + \frac{\partial^2 \psi_i}{\partial y^2} = 0, \quad i = 1, 2 \quad (7b)$$

$$\gamma^2 \frac{\partial^2 w}{\partial x^2} + \frac{\partial^2 w}{\partial y^2} = 0, \quad -h < y < 0 \quad (7c)$$

In above equations

$$c_T = \sqrt{\frac{\tilde{c}_{44}}{\rho}}, \quad \gamma = \sqrt{[G^2 - (V/C)]^2}, \quad \Gamma = \sqrt{[1 - (V/c_T)]^2}, \quad (8)$$

where c_T is the speed of the piezoelectrically stiffened bulk transverse shear wave. In this case, the boundary conditions of the problem take the form

$$\begin{aligned} \sigma_{yz}(x, h_1) &= 0, \quad \sigma_{yz}(x, -(h + h_2)) = 0, \\ D_y(x, h_1) &= 0, \quad D_y(x, -(h + h_2)) = 0, \end{aligned} \quad (9)$$

The continuity and dislocation conditions can be written as:

$$\begin{aligned} D_y(x, 0^+) &= 0, \quad \sigma_{yz}(x, 0^+) = \sigma_{yz}(x, 0^-), \\ w_1(x, 0^+) &= w(x, 0^-), \quad w(x, -h^+) = w_2(x, -h^-), \\ \sigma_{yz}(x, -h^+) &= \sigma_{yz}(x, -h^-), \quad \sigma_{yz}(x, \eta^+) = \sigma_{yz}(x, \eta^-), \\ w(x, \eta^-) - w(x, \eta^+) &= b_{wz} H(x - \xi) \quad |x| < \infty. \end{aligned} \quad (10)$$

where $H(\cdot)$ is the Heaviside-step function. The superscripts ξ^+ and ξ^- refer to the upper and lower edges of the cut, respectively. To solve the problem, Fourier transformation is introduced:

$$f^*(s) = \int_{-\infty}^{\infty} f(x) e^{isx} dx, \quad f(x) = \frac{1}{2\pi} \int_{-\infty}^{\infty} f^*(s) e^{-isx} ds, \quad (11)$$

Application of the Fourier transform to the Eqs. (7), we obtain:

$$\begin{aligned} w_1^*(s, y) &= A_1(s) \sinh(s\Gamma y) + A_2(s) \cosh(s\Gamma y), \quad 0 \leq y \leq h_1 \\ \psi_1^*(s, y) &= A_3(s) \sinh(sy) + A_4(s) \cosh(sy), \quad 0 \leq y \leq h_1 \\ w^*(s, y) &= B_1(s) \sinh(s\gamma y) + B_2(s) \cosh(s\gamma y), \quad \eta \leq y \leq 0 \\ w^*(s, y) &= B_3(s) \sinh(s\gamma y) + B_4(s) \cosh(s\gamma y), \quad -h \leq y \leq \eta \\ w_2^*(s, y) &= C_1(s) \sinh(s\Gamma y) + C_2(s) \cosh(s\Gamma y), \quad -(h+h_2) \leq y \leq -h \\ \psi_2^*(s, y) &= C_3(s) \sinh(sy) + C_4(s) \cosh(sy), \quad -(h+h_2) \leq y \leq -h \end{aligned} \quad (12)$$

Superscript $*$ and s denote Fourier transform domain and Fourier transform parameter, respectively. In the above expressions, $A_i(s), B_i(s), C_i(s), (i = 1, 2, 3, 4)$ are the unknown coefficients which will be determined from the conditions (9) and (10). Next, by using the coefficients, a simple calculations leads to the stress field in the orthotropic layer:

$$\begin{aligned} \sigma_{zy}(x, y) &= \frac{\gamma G_y b_{wz}}{2\pi} \int_0^{+\infty} \sin[s(x - \xi)] \frac{\beta \Gamma \sinh(s\Gamma h_1) \cosh(s\gamma y) - \gamma G_y \cosh(s\Gamma h_1) \sinh(s\gamma y)}{\Delta(s)} \\ &\quad \times \{(\beta \Gamma - \gamma G_y) \sinh[s(\gamma(\eta + h) + \Gamma(2h + h_2))] - (\beta \Gamma + \gamma G_y) \\ &\quad \times \sinh[s(\gamma(\eta + h) - \Gamma(2h + h_2))]\} ds \quad \eta \leq y \leq 0 \\ \sigma_{zy}(x, y) &= \frac{\gamma G_y b_{wz}}{2\pi} \int_0^{+\infty} \sin[s(x - \xi)] \frac{\beta \Gamma \sinh(s\Gamma h_1) \cosh(s\gamma \eta) - \gamma G_y \cosh(s\Gamma h_1) \sinh(s\gamma \eta)}{\Delta(s)} \\ &\quad \times \{(\beta \Gamma - \gamma G_y) \sinh[s(\gamma(y + h) + \Gamma(2h + h_2))] - (\beta \Gamma + \gamma G_y) \\ &\quad \times \sinh[s(\gamma(y + h) - \Gamma(2h + h_2))]\} ds, \quad -h \leq y \leq \eta \end{aligned} \quad (13)$$

where $\alpha = e_{15}^2 + d_{11}c_{44}$, $\beta = G_y g_{d11}$. The expressions for $\Delta(s)$ is given by:

$$\begin{aligned} \Delta(s) &= \gamma G_y [\beta \Gamma \cosh(s\gamma h) \sinh[s\Gamma(2h + h_2)] \cosh(s\Gamma h_1) - \beta \Gamma \cosh(s\gamma h) \\ &\quad \times \cosh[s\Gamma(2h + h_2)] \sinh(s\Gamma h_1) - \gamma G_y \cosh[s\Gamma(2h + h_2)] \cosh(s\Gamma h_1) \sinh(s\gamma h)] \\ &\quad + \beta^2 \Gamma^2 \sinh(s\gamma h) \sinh[s\Gamma(2h + h_2)] \sinh(s\Gamma h_1) \end{aligned} \quad (14)$$

The integrals in Eq. (13) diverge in the vicinity of dislocation. To circumvent this difficulty, the singular nature of the stress field must be examined. It may be seen that the integrals in Eq. (13) are bounded at $s = 0$. If we further observe that the integrands in Eq. (13) are continuous functions of s , it is then clear that any singularity of the kernels may have must be due to the asymptotic behavior of the integrands as s approaches infinity.

The singular parts may be evaluated by the use of following identities:

$$\int_0^{\infty} e^{sy} \sin(sx) ds = \frac{x}{x^2 + y^2}, \quad y < 0$$

$$\int_0^{\infty} e^{sy} \cos(sx) ds = -\frac{y}{x^2 + y^2}, \quad y < 0$$
(15)

By adding and subtracting the asymptotic expressions of the integrands obtained by using Eqs. (15) we find:

$$\begin{aligned} \sigma_{zy}(x, y) = & \frac{\gamma G_y b_{wz}}{2\pi} \frac{(x - \xi)}{(x - \xi)^2 + \gamma^2(\eta - y)^2} \\ & + \frac{\gamma G_y b_{wz}}{2\pi} \int_0^{+\infty} \sin[s(x - \xi)] \left\{ \frac{\beta \Gamma \sinh(s \Gamma h_1) \cosh(s \gamma y) - \gamma G_y \cosh(s \Gamma h_1) \sinh(s \gamma y)}{\Delta(s)} \right. \\ & \times ((\beta \Gamma - \gamma G_y) \sinh[s(\gamma(\eta + h) + \Gamma(2h + h_2))] - (\beta \Gamma + \gamma G_y) \\ & \times \sinh[s(\gamma(\eta + h) - \Gamma(2h + h_2))]) - e^{s\gamma(\eta - y)} \} ds \\ \sigma_{zy}(x, y) = & \frac{\gamma G_y b_{wz}}{2\pi} \frac{(x - \xi)}{(x - \xi)^2 + \gamma^2(\eta - y)^2} \\ & + \frac{\gamma G_y b_{wz}}{2\pi} \int_0^{+\infty} \sin[s(x - \xi)] \left\{ \frac{\beta \Gamma \sinh(s \Gamma h_1) \cosh(s \gamma \eta) - \gamma G_y \cosh(s \Gamma h_1) \sinh(s \gamma \eta)}{\Delta(s)} \right. \\ & \times ((\beta \Gamma - \gamma G_y) \sinh[s(\gamma(y + h) + \Gamma(2h + h_2))] - (\beta \Gamma + \gamma G_y) \\ & \times \sinh[s(\gamma(y + h) - \Gamma(2h + h_2))]) - e^{s\gamma(y - \eta)} \} ds \end{aligned}$$
(16)

We may observe that stress components exhibit the familiar Cauchy type singularity at the dislocation location. Again, for large values of s the integrals in Eq. (16) become unbounded. The integrations in Eq. (16) should be performed differently.

Finally, stress components may be expressed as:

$$\begin{aligned} \sigma_{zy}(x, y) = & \frac{\gamma G_y b_{wz}}{2\pi} \left\{ \frac{(x - \xi)}{(x - \xi)^2 + \gamma^2(\eta - y)^2} \right. \\ & + \int_0^{+\infty} e^{s\gamma(\eta - y)} \sin[s(x - \xi)] \left\{ \frac{\beta \Gamma (1 - e^{-2s\Gamma h_1})(e^{2s\gamma y} + 1) - \gamma G_y (1 + e^{-2s\Gamma h_1})(e^{2s\gamma y} - 1)}{\Delta'(s)} \right. \\ & \times [(\beta \Gamma - \gamma G_y)(1 - e^{-2s\gamma \eta} e^{-2s[\gamma h + \Gamma(2h + h_2)]}) - (\beta \Gamma + \gamma G_y)(e^{-2s[\Gamma(2h + h_2)]} - e^{-2s\gamma(\eta + h)})] - 1 \} ds \\ \sigma_{zy}(x, y) = & \frac{\gamma G_y b_{wz}}{2\pi} \left\{ \frac{(x - \xi)}{(x - \xi)^2 + \gamma^2(\eta - y)^2} \right. \\ & + \int_0^{+\infty} e^{s\gamma(y - \eta)} \sin[s(x - \xi)] \left\{ \frac{\beta \Gamma (1 - e^{-2s\Gamma h_1})(e^{2s\gamma \eta} + 1) - \gamma G_y (1 + e^{-2s\Gamma h_1})(e^{2s\gamma \eta} - 1)}{\Delta'(s)} \right. \\ & \times \{ (\beta \Gamma - \gamma G_y)(1 - e^{-2s\gamma y} e^{-2s[\gamma h + \Gamma(2h + h_2)]}) - (\beta \Gamma + \gamma G_y)(e^{-2s[\Gamma(2h + h_2)]} - e^{-2s\gamma(y + h)}) \} - 1 \} ds \end{aligned}$$
(17)

where

$$\begin{aligned} \Delta'(s) = & \gamma G_y [\beta \Gamma (1 + e^{-2s\gamma h})(1 - e^{-2s\Gamma(2h+h_2)})(1 + e^{-2s\Gamma h_1}) - \beta \Gamma (1 + e^{-2s\gamma h})(1 + e^{-2s\Gamma(2h+h_2)})(1 - e^{-2s\Gamma h_1}) \\ & - \gamma G_y (1 + e^{-2s\Gamma(2h+h_2)})(1 + e^{-2s\Gamma h_1})(1 - e^{-2s\gamma h})] + \beta^2 \Gamma^2 (1 - e^{-2s\Gamma(2h+h_2)})(1 - e^{-2s\Gamma h_1})(1 - e^{-2s\gamma h}) \end{aligned} \quad (18)$$

For computational efficiency it may also be more convenient. All integrals in Eq. (17) decay sufficiently rapidly as $s \rightarrow \infty$, which makes the integrals susceptible to numerical evaluation.

3 Solutions to moving cracks

The dislocation solutions obtained in the previous section is not restricted to single crack problems. It can be used to analyze layers containing multiple moving cracks. We consider an orthotropic layer weakened by N arbitrary moving cracks. The cracks configuration may be described in parametric form as

$$\begin{aligned} x_i &= x_{0i}(s) + L_i s \\ y_i &= y_{0i}(s) \quad i \in \{1, 2, \dots, N\}, \quad -1 \leq s \leq 1 \end{aligned} \quad (19)$$

suppose dislocations with unknown density $B_{zj}(t)$ are distributed on the infinitesimal segment dL_j at the surface of j -th crack. The traction components on the surface of the i -th crack due to the presence of above-mentioned distribution of dislocations on the surfaces of all N cracks yield:

$$\sigma_{zn}(x_i(s), y_i(s)) = \sum_{j=1}^N \int_{-1}^1 K_{ij}(s, t) B_{zj}(t) L_j dt \quad i = 1, 2, \dots, N. \quad (20)$$

where $B_{zj}(t)$ are the dislocation densities on the nondimensionalized length $-1 \leq t \leq 1$. The kernel of integral equations (20) take the form:

$$\begin{aligned} K_{ij} = & \frac{\gamma G_y}{2\pi} \left\{ \frac{(x_i - x_j)}{(x_i - x_j)^2 + \gamma^2 (y_j - y_i)^2} \right. \\ & + \int_0^{+\infty} e^{s\gamma(y_j - y_i)} \sin[s(x_i - x_j)] \left\{ \frac{\beta \Gamma (1 - e^{-2s\Gamma h_1})(e^{2s\gamma y_i} + 1) - \gamma G_y (1 + e^{-2s\Gamma h_1})(e^{2s\gamma y_i} - 1)}{\Delta'(s)} \right. \\ & \times [(\beta \Gamma - \gamma G_y)(1 - e^{-2s\gamma y_j} e^{-2s[\gamma h + \Gamma(2h+h_2)]}) - (\beta \Gamma + \gamma G_y)(e^{-2s[\Gamma(2h+h_2)]} - e^{-2s\gamma(y_j+h)})] - 1 \} ds \\ & \left. \left. \times \{ (\beta \Gamma - \gamma G_y)(1 - e^{-2s\gamma y_i} e^{-2s[\gamma h + \Gamma(2h+h_2)]}) - (\beta \Gamma + \gamma G_y)(e^{-2s[\Gamma(2h+h_2)]} - e^{-2s\gamma(y_i+h)}) \} - 1 \} ds \right. \right. \\ & \left. \left. y_j \leq y \leq 0 \right. \right. \\ \\ K_{ij} = & \frac{\gamma G_y}{2\pi} \left\{ \frac{(x_i - x_j)}{(x_i - x_j)^2 + \gamma^2 (y_j - y_i)^2} \right. \\ & + \int_0^{+\infty} e^{s\gamma(y_i - y_j)} \sin[s(x_i - x_j)] \left\{ \frac{\beta \Gamma (1 - e^{-2s\Gamma h_1})(e^{2s\gamma y_j} + 1) - \gamma G_y (1 + e^{-2s\Gamma h_1})(e^{2s\gamma y_j} - 1)}{\Delta'(s)} \right. \\ & \times \{ (\beta \Gamma - \gamma G_y)(1 - e^{-2s\gamma y_i} e^{-2s[\gamma h + \Gamma(2h+h_2)]}) - (\beta \Gamma + \gamma G_y)(e^{-2s[\Gamma(2h+h_2)]} - e^{-2s\gamma(y_i+h)}) \} - 1 \} ds \\ & \left. \left. - h \leq y \leq y_j \right. \right. \end{aligned} \quad (21)$$

The left hand side of the Eqs. (20) are stress components at the presumed location of the moving crack with negative sign. Employing the definition of dislocation density functions, the equations for the crack opening displacement across j -th crack become:

$$w_j^+(s) - w_j^-(s) = \int_{-1}^s B_{zj}(t) L_j dt \quad j = 1, 2, \dots, N. \quad (22)$$

The displacement field is single-valued out of surfaces of moving cracks. Consequently, Cauchy singular integral Eqs. (20) should be complemented by closure requirements

$$L_j \int_{-1}^1 B_{zj}(t) dt = 0, \quad j = 1, 2, \dots, N. \quad (23)$$

The singular integral equations (20) are solved numerically by using (23) and an appropriate collocation technique to determine dislocation density functions. Therefore, the dislocation density function, $B_{zj}(t)$, having the square root singularity at the crack tips, can be expressed as:

$$B_{zj}(t) = \frac{g_{zj}(t)}{\sqrt{1-t^2}}, \quad -1 \leq t \leq 1, \quad j = 1, 2, \dots, N. \quad (24)$$

The stress intensity factors at the tip of i -th crack in terms of the crack opening displacement reduce to:

$$K_{Li} = \frac{\sqrt{2}}{4} \sqrt{G_{zx} G_{zy}} \lim_{r_{Li} \rightarrow 0} \frac{w_i^-(s) - w_i^+(s)}{\sqrt{r_{Li}}},$$

$$K_{Ri} = \frac{\sqrt{2}}{4} \sqrt{G_{zx} G_{zy}} \lim_{r_{Ri} \rightarrow 0} \frac{w_i^-(s) - w_i^+(s)}{\sqrt{r_{Ri}}} \quad (25)$$

where L and R designate, the left and right tips of a cracks, respectively. The function $g_{zj}(t)$ are obtained via solution of the system of equations. The stress intensity factors for the i -th crack are defined by:

$$K_{Lj} = \frac{GG_y}{2} \left[[x'_j(-1)]^2 + [y'_j(-1)]^2 \right]^{\frac{1}{4}} g_{zj}(-1)$$

$$K_{Rj} = -\frac{GG_y}{2} \left[[x'_j(1)]^2 + [y'_j(1)]^2 \right]^{\frac{1}{4}} g_{zj}(1) \quad (26)$$

The details of the derivation of fields intensity factors to reach (26) are not given here. According to the theory of strain energy density criterion [20,21], the strain energy density factor S at the crack tip for the model III crack of orthotropic composites can be expressed as:

$$S = \frac{K_{III}^2}{4\pi G_x} \sin^2 \frac{\theta}{2} + \frac{K_{III}^2}{4\pi G_y} \cos^2 \frac{\theta}{2} \quad (27)$$

Referring to the strain energy density criterion, the minimum value of S can be obtained as follows:

$$\frac{\partial S}{\partial \theta} = 0 \quad (28)$$

Substituting Eq. (27) into (28), it is found that $\theta = 0$ and $\theta = \pi$

$$S_{\min} = \frac{K_R^2}{4G_y} \quad G_x < G_y, \quad \theta_0 = 0$$

$$S_{\min} = \frac{K_L^2}{4G_x} \quad G_x > G_y, \quad \theta_0 = \pi. \quad (29)$$

where θ_0 is the angle of crack initiation. Eq. (27) can be made dimensionless by dividing by

$$S_0 = \frac{\tau_0^2 L}{4G_y}, \text{ i.e.,}$$

$$\frac{S_{\min}}{(\tau_0^2 L)/4G_y} = \frac{G_x G_y}{4\tau_0^2} [g_{zj}(1)]^2$$

$$\frac{S_{\min}}{(\tau_0^2 L)/4G_y} = \frac{G_y^2}{4\tau_0^2} [g_{zj}(-1)]^2, \quad j=1,2,\dots,N \quad (30)$$

4 Results and discussions

In this section we are mainly concerned with the determination of the dynamic stress intensity and strain energy density factors. The proposed approach makes it possible to consider an orthotropic strip bonded between two piezoelectric layers with multiple moving cracks. The thickness of each piezoelectric layer is normalized with respect to the thickness of the orthotropic layer. The medium is assumed to be loaded by constant tractions with the magnitude of τ_0 which are distributed on the boundaries.

It should be noted that through the paper, divisor $K_0 = \tau_0 \sqrt{L}$, with L being the half length of crack, is used to make the crack stress intensity factors dimensionless. We can take PZT-4 ceramic as an example of which the engineering material constants are given by

$$c_{44} = 2.56 \times 10^{10} \left(\frac{N}{m^2} \right), e_{15} = 12.7 \left(\frac{C}{m^2} \right), d_{11} = 64.6 \times 10^{-10} \left(\frac{C}{Vm} \right), \rho = 7.5 \times 10^3 \left(\frac{kg}{m^3} \right), \quad (31)$$

The verification is accomplished by comparing the stress intensity factor of a stationary crack by approaching h to infinity and satisfies $K/K_0 = 1.0$ which agrees well with the previous result of Singh et al. [22], see Figure (2). It is worth noting that, in case the thickness of orthotropic layer goes to infinity the stress intensity factor is not changed.

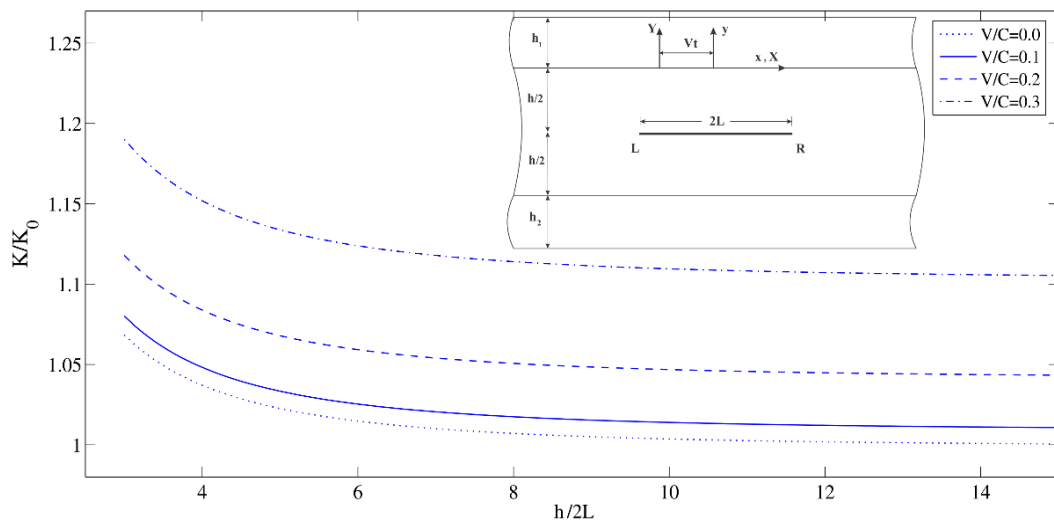


Figure 2 Normalized stress intensity factor versus $h/2L$ for different crack speed.

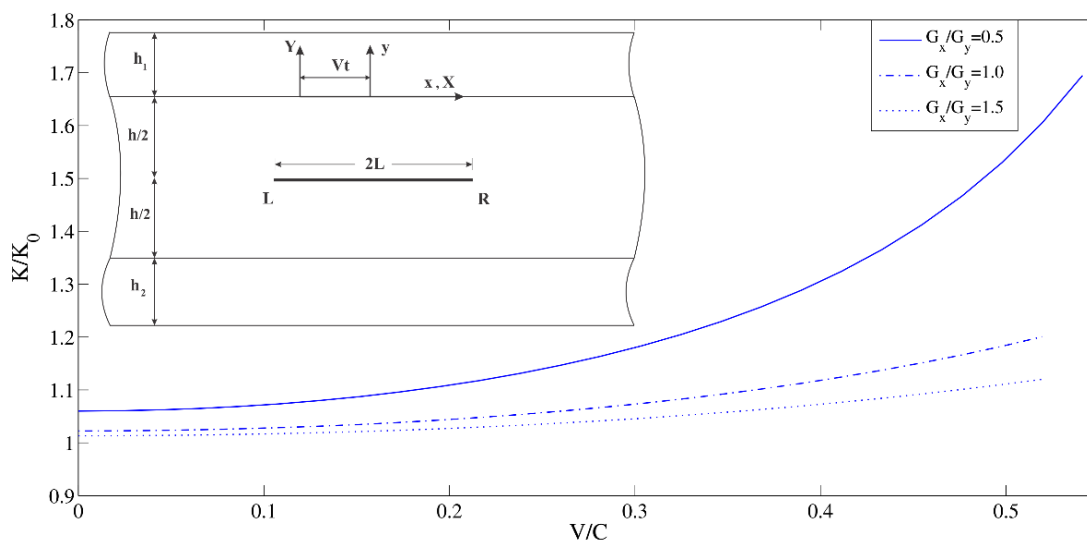


Figure 3 Normalized stress intensity factor versus dimensionless crack speed for different ratios of shear moduli.

The variation of normalized stress intensity factors K/K_0 with the velocity of crack for different ratios of shear moduli is shown in Figure (3). It can be clear that, the problem is symmetric with respect to the y-axis, the thickness of the two piezoelectric layers are taken as $h_1 = h_2 = 0.25h$. The crack length is assumed as $2L = 1.25h$. It can be found that, the stress intensity factor increases with increasing the crack speed. It is worth noting that, the stress intensity factors are significantly influenced by changing the values of the ratios of shear moduli. Figure (4) displays the variations of normalized strain energy density factor with the normalized crack velocity for three different ratios of moduli. In all cases, it can be observed that the magnitude of S_{\min}/S_0 increases with the increasing of the crack speed and decreases with increasing the ratios of shear moduli.

Figure (5) shows the normalized stress intensity factor, K/K_0 , as a function of the normalized crack position, H/h , for varying normalized crack speeds.

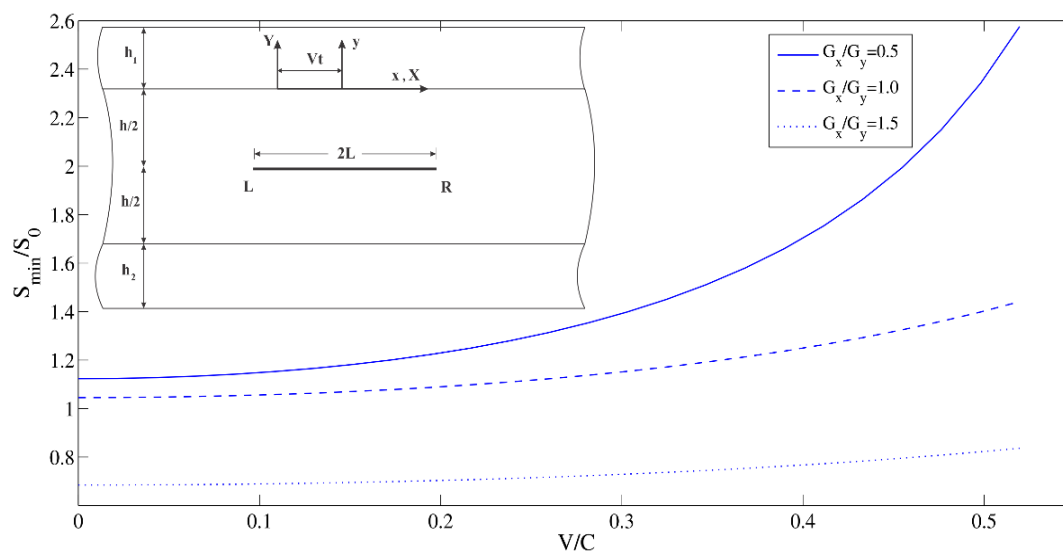


Figure 4 Variation of normalized strain energy density factor versus dimensionless crack speed for different ratio of the shear moduli.

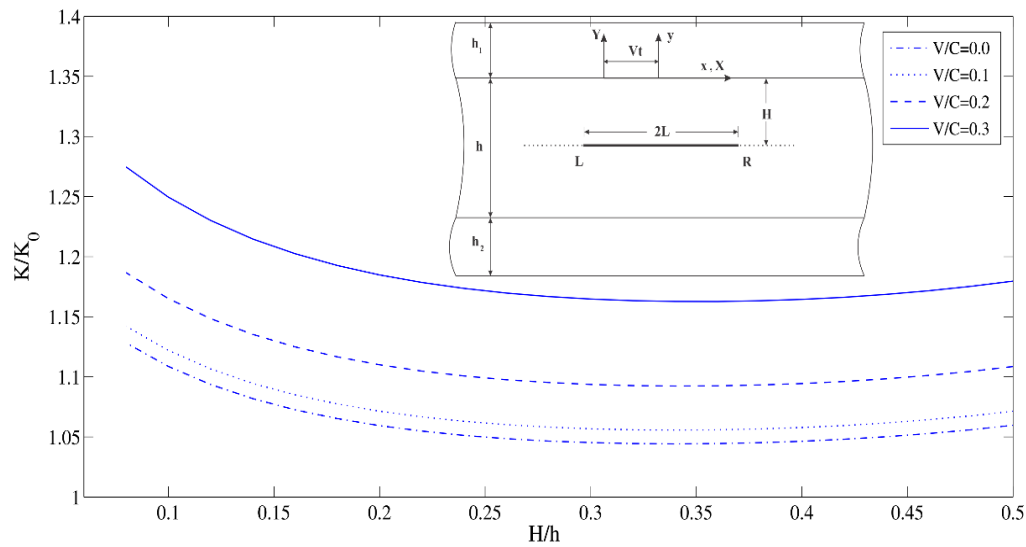


Figure 5 Normalized stress intensity factor versus the ratio H/h .

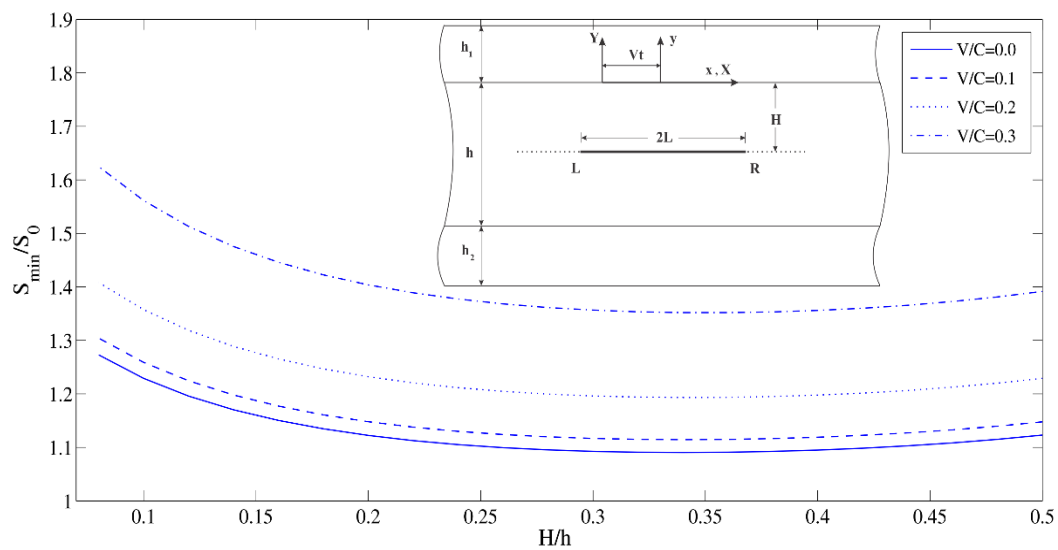


Figure 6 Variation of normalized strain energy density factor with crack position for different V/C values.

Similar analysis can be made for Figure (6), which presents the variations of normalized strain energy density factor, S_{\min}/S_0 , versus crack position. On the other hand, if the crack velocity is constant, the ratios of the shear moduli and crack position have great influence on the strain energy density factor of the moving crack. In these examples, the ratios of shear moduli is chosen $G_x/G_y = 0.5$. In the next example, we consider two collinear equal-length moving cracks which are located on the the center-line of the orthotropic strip.

Figure (7) shows the normalized stress intensity factor, K/K_0 as a function of crack speed for various values of the ratios of shear moduli of orthotropic strip. For all cases, stress intensity factors increase as the cracks velocity increase under anti-plane loading.

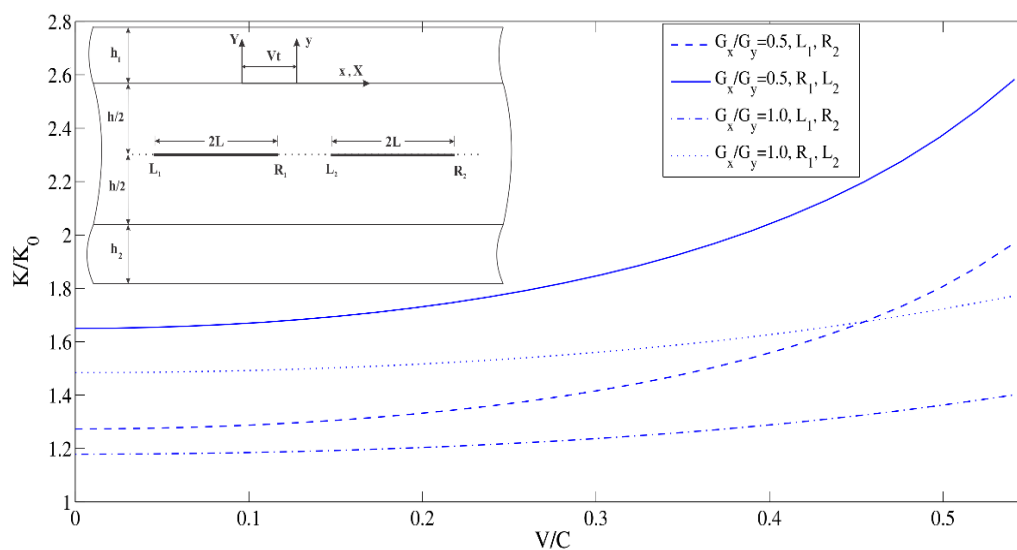


Figure 7 Normalized stress intensity factor versus the dimensionless crack speed for different ratio of the shear moduli.

The influence of the material parameter G_x/G_y on the stress intensity factors could be quite significant. In the case of coaxial cracks, due to symmetry, the stress intensity factors L_1 and R_1 are equal to those at R_2 and L_2 , respectively.

Figure (8) shows the variation of stress intensity factor, K/K_0 versus the geometric size ratios L/d for different case of crack velocity. We keep the distance the crack centers constant and increase the crack length. The stress intensity factors increases as the ratio L/d increases. As it was expected, the stress intensity factors are increased with increasing the crack length. In this example, the value of the ratios of the shear moduli is chosen $G_x/G_y = 0.5$. The trend of variation remain the same by changing the ratios of shear moduli.

The variation of stress intensity factors of two interacting crack tips namely R_1 and L_2 is more pronounced than that of the tips L_1 and R_2 . Obviously, Approaching the crack tips leads to the more interactions and then K/K_0 , are increased.

The next example deals with the interaction of two off-centers equal length cracks which are parallel to the strip edges. The centers of cracks remain fixed while the crack length are changing with the same rate. The normalized stress intensity factors versus crack length are depicted in Figure (9). As it might be observed the maximum stress intensity factors for the crack tips R_1 and L_2 occur when the distance between them is minima.

The orthotropic strip contains two parallel identical moving cracks with length $2L$ which are also parallel with strip edges. The crack L_1R_1 is located on the strip center-line and the crack L_2R_2 is situated at the vertical distance H below the interface of the layers.

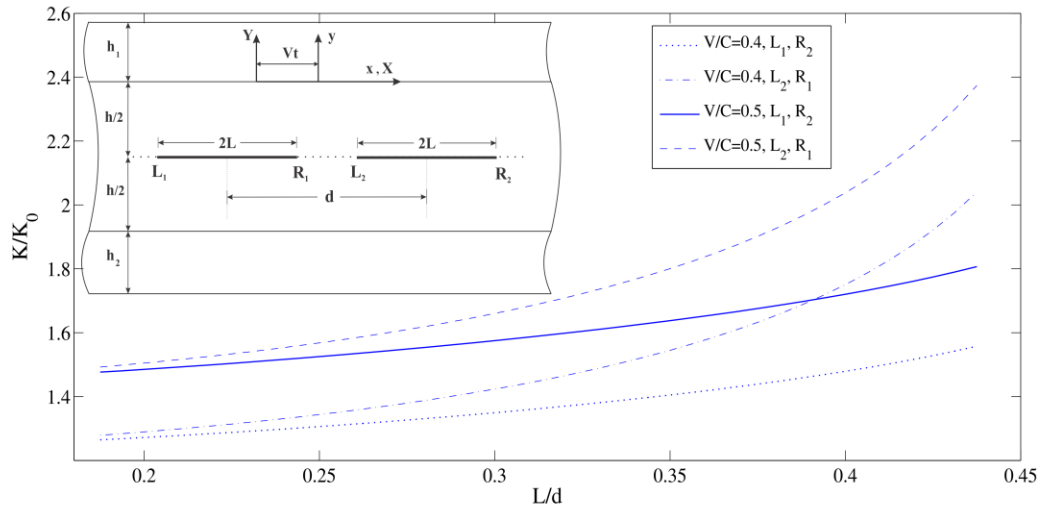


Figure 8 Variation of normalized stress intensity factors with L/d .

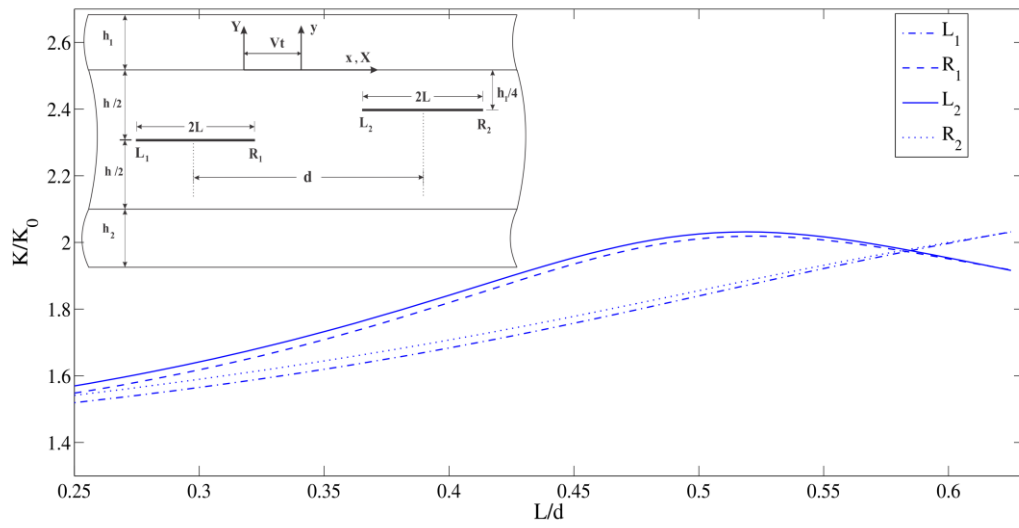


Figure 9 Normalized stress intensity factors of crack tips versus the dimensionless crack length.

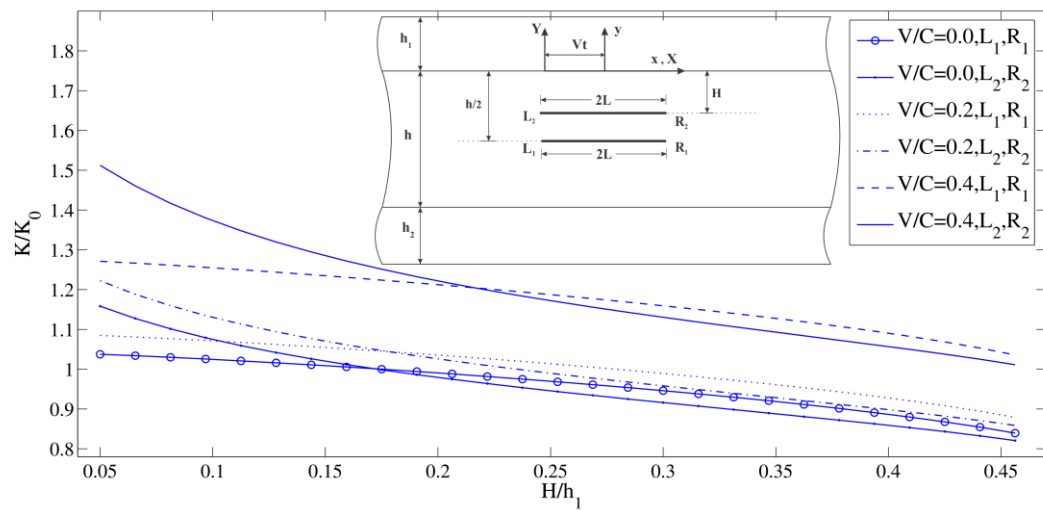


Figure 10 Normalized stress intensity factor versus H/h for different dimensionless crack speed.

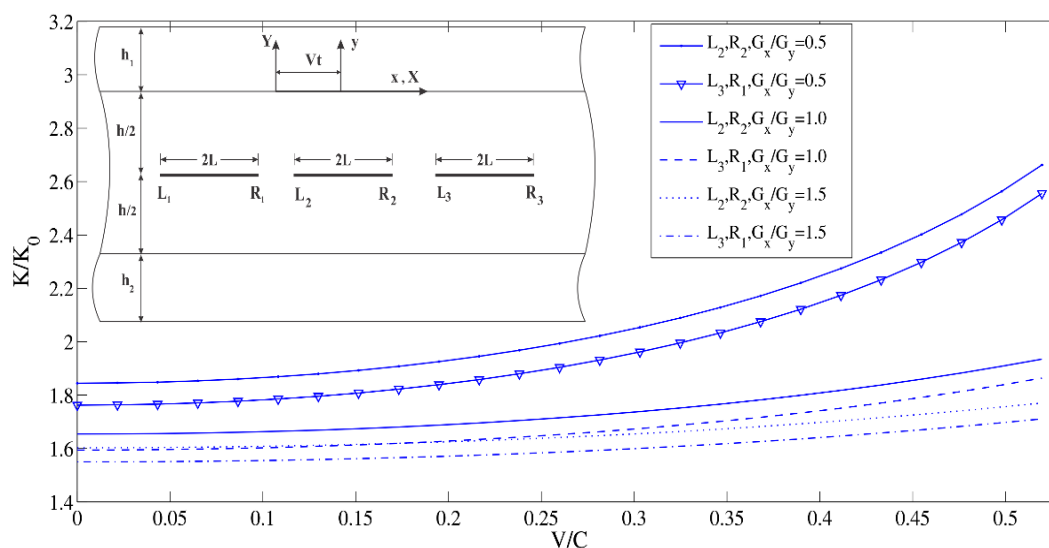


Figure 11 Normalized stress intensity factors of crack tips versus the dimensionless crack speed.

Figure (10) shows the normalized stress intensity factors as a function of the normalized crack location, for change of the crack velocity. In this case, the stress intensity factors increases with an increase in crack speed regardless of the crack location.

Figure (11) shows the variations of the normalized stress intensity factors with the normalized crack velocity V/C for different ratios of shear moduli. A significant increase in K/K_0 is observed with an increase in crack speed.

5 Conclusions

The solution of screw dislocation is obtained in an orthotropic strip bonded between two piezoelectric layers. The dislocation solution is utilized to perform the integral equations for the orthotropic strip with moving crack. These equations are of Cauchy singular type solvable by numerical methods to obtain dislocation density on the moving crack surfaces.

To study the intractions between the cracks, and also the effect of crack speed, stress intensity factors are obtained for some examples. The results show that, in addition to the influences of the crack geometry on the stress intensity factors (as expected), the crack speed is also be very significant.

References

- [1] Sih, G. C., and Chen, E. P., "Moving Cracks in Layered Composites", International Journal of Engineering Sciences, Vol. 20, pp. 1181–1192, (1982).
- [2] Chen, Z.T., Karihaloo, B.L., and Yu, S.W., "A Griffith Crack Moving Along the Interface of Two Dissimilar Piezoelectric Materials", International Journal of Fracture Vol. 91, pp. 197–203, (1998).
- [3] Kwon, J.H., and Lee, K.Y., "Interface Crack between Piezoelectric and Elastic Strips", Archives of Applied Mechanics, Vol. 70, pp. 707-714, (2000).

- [4] Das, S., Patra, B., and Debnath, L., "Stress Intensity Factors around Two Co-planar Griffith Cracks in an Orthotropic Layer Sandwiched between Two Identical Orthotropic Half-planes", *International Journal of Engineering Sciences*, Vol. 38, pp. 121-133, (2000).
- [5] Kwon, J.H., and Lee, K.Y., "Moving Interfacial Crack between Piezoelectric Ceramic and Elastic Layers", *European Journal of Mechanics- A/Solids*, Vol. 19, pp. 979-987, (2000).
- [6] Jiang, L.Y., and Wang, X.D., "On the Dynamic Propagation in an Interphase with Spatially Varying Elastic Properties under In-plane Loading", *International Journal of Fracture* Vol. 114, pp. 225-244, (2002).
- [7] Kwon, S.M., Lee, J.S., and Lee, K.Y., "Moving Eccentric Crack in a Piezoelectric Strip Bonded to Elastic Half-planes", *International Journal of Solids and Structures*, Vol. 39, pp. 4395-4406, (2002).
- [8] Lee, J.S., Kwon, S.M., Lee, K.Y., and Kwon, H., "Anti-plane Interfacial Yoffe-crack between a Piezoelectric and Two Orthotropic Layers", *European Journal of Mechanics-A/Solids*, Vol. 21, pp. 483-492, (2002).
- [9] Kwon, S.M., Son, M.S., and Lee, K.Y., "Transient Behavior in a Cracked Piezoelectric Layered Composite: Anti-plane Problem", *Mechanics of Materials*, Vol. 34, pp. 593-603, (2002).
- [10] Chi, S., and Chung, Y.L., "Cracking in Coating-substrate Composites with Multi-layered and FGM Coating", *Engineering Fracture Mechanics*, Vol. 70, pp. 1227-1243, (2003).
- [11] Ma, L., Wu, L.Z., and Guo, L.C., "On the Moving Griffith Crack in a Non-homogeneous Orthotropic Strip", *International Journal of Fracture*, Vol. 136, pp. 187-205, (2005).
- [12] Das, S., "Interaction of Moving Interface Collinear Griffith Cracks under Antiplane Shear", *International Journal of Solids and Structures*, Vol. 43, pp. 7880-7890, (2006).
- [13] Cheng, Z., and Zhong, Z., "Analysis of a Moving Crack in a Functionally Graded Strip between Two Homogeneous Layers", *International Journal of Mechanical Sciences*, Vol. 49, pp. 1038-1046, (2007).
- [14] Matbully, M.S., "Multiple Crack Propagation Along the Interface of a Non-homogeneous Composite Subjected to Anti-plane Shear Loading", *Meccanica*, Vol. 44, pp. 547-554, (2009).
- [15] Li, X., and Ding, S.H., "Periodically Distributed Parallel Cracks in a Functionally Graded Piezoelectric (FGP) Strip Bonded to a FGP Substrate under Static Electromechanical Load", *Computational Materials Science*, Vol. 50, pp. 1477-1484, (2009).
- [16] Feng, F.X., Lee, K.Y., and Li, Y.D., "Multiple Cracks on the Interface between a Piezoelectric Layer and an Orthotropic Substrate", *Acta Mechanica*, Vol. 221, pp. 297-308, (2011).

- [17] Shin, J.W., and Lee, Y.S., "Anti-plane Moving Crack in a Functionally Graded Piezoelectric Layer between Two Dissimilar Piezoelectric Strips", *Journal of Mechanical Science and Technology*, Vol. 26, pp. 1017-1025, (2012).
- [18] Ding, S.H., and Li, X., "The Collinear Crack Problem for an Orthotropic Functionally Graded Coating-substrate Structure", *Archives of Applied Mechanics*, Vol. 84, pp. 291-307, (2014).
- [19] Erdogan, F., and Gupta, G.D., "On the Numerical Solution of Singular Integral Equations", *Quarterly of Applied Mathematics*. Vol. 29, pp. 525-534, (1972).
- [20] Sih, G.C., "A Three-dimensional Strain Energy Density Theory of Crack Propagation: Three-dimensional of Crack Problems", in: G.C. Sih (Ed.), *Mechanics of Fracture II*, Noordhoof International Publishing, Leyden, pp. 15-53, (1975).
- [21] Sih, G.C., "*Mechanics of Fracture Initiation and Propagation*", Kluwer, Boston, (1991).
- [22] Singh, B.M., Moodie, T.B., and Haddow, J.B., "Closed-form Solutions for Finite Length Crack Moving in a Strip under Anti-plane Shear Stress", *Acta Mechanica*, Vol. 38, pp. 99-109, (1981).

Nomenclature

A_i, B_i, C_i	Unknown coefficients
b_{wz}	Burger vector
$B_{zj}(t)$	Dislocation density function
c_{44}	Elastic constant
C	Elastic shear wave velocity
d_{11}	Dielectric permittivity
D_{Xi}, D_{Yi}	Electric displacement components
G_X, G_Y	Orthotropic shear moduli
h	Thickness of orthotropic strip
h_1, h_2	Thickness of piezoelectric layers
$H(x)$	Heaviside step function
$K_{ij}(s, t)$	Kernel of integral equations
K_{Li}, K_{Ri}	Stress intensity factors of left and right side of crack
K_0	Stress intensity factor of a crack in infinite plane
L	Half length of crack
N	Number of cracks
S	Strain energy density
W	Anti-plane displacement
x, y	Translating coordinates
ϕ	Electric potential
ρ	Mass density
σ_{zx}, σ_{zy}	Stress components

چکیده

در این مقاله حل نابجایی متحرک در لایه ارتوتروپیک متصل به دو لایه پیزوالکتریک با استفاده از تبدیل فوریه بدست آمده است. سپس به کمک روش توزیع نابجایی معادلات با تکینگی کوشی برای محیط حاوی چندین ترک متحرک بدست آمده است. با حل عددی معادلات انتگرالی و محاسبه دانسیته نابجایی بر روی سطوح ترک های متحرک، از آن برای محاسبه ضرایب شدت تنش استفاده شده است. در نهایت اثر خواص مواد پارامترهای هندسی بر روی ضرایب شدت تنش و شدت انرژی کرنشی ارائه شده است.